Short Communication

Continuous hydrogenation of hydroquinone to 1,4-cyclohexanediol over alkaline earth metal modified nickel-based catalysts

Guoyi Bai *, Fei Li, Xinxin Fan, Yalong Wang, Mande Qiu, Zheng Ma, Libo Niu

Key Laboratory of Medicinal Chemistry and Molecular Diagnosis of Ministry of Education, College of Chemistry and Environmental Science, Hebei University, Baoding, Hebei, 071002, PR China

ARTICLE INFO

ABSTRACT

Effects of different alkaline earth metals (Mg, Ca, Sr) on the nickel-based catalysts for the continuous hydrogenation of hydroquinone were studied, and it was found that the by-products, characterized by GC–MS analysis, were mainly composed of phenol and cyclohexanol. The conversion of hydroquinone was 99.2% and the selectivity to 1,4-cyclohexanediol was above 96.7% over a Ni–Sr/γ-Al$_2$O$_3$ catalyst at 160 °C and 2.0 MPa hydrogen pressure. The high selectivity of the Ni–Sr/γ-Al$_2$O$_3$ catalyst was ascribed to its weak acidity due to the formation of SrCO$_3$, confirmed from XRD and NH$_3$-TPD characterizations. Moreover, it was proposed that SrCO$_3$ can disperse and stabilize the active Ni species, making the catalyst stable during the 90 h service life test.

1. Introduction

1,4-Cyclohexanediol is an important intermediate for the synthesis of medicinal and liquid crystal materials [1,2]. Traditionally, 1,4-cyclohexanediol was produced mainly by the hydrogenation of hydroquinone using Ni/SiO$_2$ [3], Raney Ni [4] or noble metal catalysts [5]. For example, Adkins and Cramer first reported the synthesis of 1,4-cyclohexanediol from the hydrogenation of hydroquinone over a Ni/SiO$_2$ catalyst, but no data on the catalyst stability were provided [3]. The reported methods were all batch process and lack of efficiency, and the catalysts used either caused serious environmental pollution or were of high cost. Therefore, it is desirable to develop a novel method for the effective synthesis of 1,4-cyclohexanediol.

Although nickel-based catalysts have been widely used in industry for the continuous hydrogenation of compounds with phenol structures [6,7], no work has ever been reported about the continuous hydrogenation of hydroquinone due to its complex structure as well as lacking more effective and stable catalysts. In this study, we first investigated the continuous hydrogenation of hydroquinone to 1,4-cyclohexanediol over nickel-based catalysts. Considering that the acidity of the catalysts may cause the dehydration of hydroquinone and 1,4-cyclohexanediol [8–11], the acidic and basic capacities of the catalysts were regulated by the addition of some basic promoters, such as the alkaline earth metals (Mg, Ca, Sr). A Ni–Sr/γ-Al$_2$O$_3$ catalyst showed significantly higher activity and selectivity toward 1,4-cyclohexanediol compared with other catalysts. The structures of the nickel-based catalysts were characterized and the results were found to correlate well with their activities.

2. Experimental methods

2.1. Catalyst preparation

Unless otherwise stated, all chemicals were purchased from Baoding Huaxin Reagent and Apparatus Co., Ltd. and were used as received without further purification. The nickel-based catalysts were prepared by the co-precipitation method. A typical procedure is as follows. A solution containing requisite amounts of metal nitrates were added dropwise to a mixture of Na$_2$CO$_3$ and powder γ-Al$_2$O$_3$ (Xinxiang Jinsheng New Material Co., Ltd.) at 40 °C. The final pH value was adjusted to 8 with Na$_2$CO$_3$ solution. Then, the co-precipitated mass was thoroughly washed, filtered, dried at 110 °C for 4 h and calcined at 500 °C for 4 h. The obtained catalysts were designated as Ni/γ-Al$_2$O$_3$, Ni–Mg/γ-Al$_2$O$_3$, Ni–Ca/γ-Al$_2$O$_3$, and Ni–Sr/γ-Al$_2$O$_3$, respectively.

2.2. Catalyst characterization

The nitrogen adsorption was measured using a Micromeritics Tristar II 3020 surface area and pore analyzer. X-ray diffraction (XRD) analysis was carried out on a Y-2000 X-ray diffractometer with Cu Kα radiation. Scanning electron micrographs (SEM) were obtained on a JEOL JSM-7500 instrument. H$_2$ chemisorption, temperature programmed reduction (TPR) and temperature programmed desorption of NH$_3$ (NH$_3$-TPD) were performed using a TP-5000 instrument from Xianquan Ltd. The X-ray photoelectron spectroscopy (XPS) measurements were

* Corresponding author at: No. 180 Wusi East Road, Baoding City, Hebei 071002, PR China. Tel.: +86 312 5079359; fax: +86 312 5937102.
E-mail address: baiguoyi@hotmail.com (G. Bai).

Table 1
Physicochemical properties of the nickel-based catalysts.

Catalyst	Surface area (m^2/g)	Pore volume (cm^3/g)	Pore size (nm)	Particle sizes[a]		Ni dispersion[b] (%)	Surface atomic ratio of Ni (%)[c]
				Before reduction	After reduction		
Ni/γ-Al$_2$O$_3$	135	0.20	6.03	13.6	20.5	25.4	12.7
Ni–Mg/ γ-Al$_2$O$_3$	164	0.23	5.63	13.5	23.9	26.7	12.8
Ni–Ca/ γ-Al$_2$O$_3$	140	0.17	5.05	10.2	22.0	25.9	8.6
Ni–Sr/ γ-Al$_2$O$_3$	165	0.21	5.08	10.1	15.8	28.1	7.6

[a] Based on XRD results.
[b] Calculated from the H_2 chemisorption [12].
[c] Based on XPS results (C is excluded).

recorded with a PHI 1600 spectroscope using Mg Kα X-ray source for excitation.

2.3. Catalyst activity test

Hydrogenation of hydroquinone was carried out in a tubular, fixed-bed reactor with 15 mm i.d., and 5.0 g catalyst was loaded into this
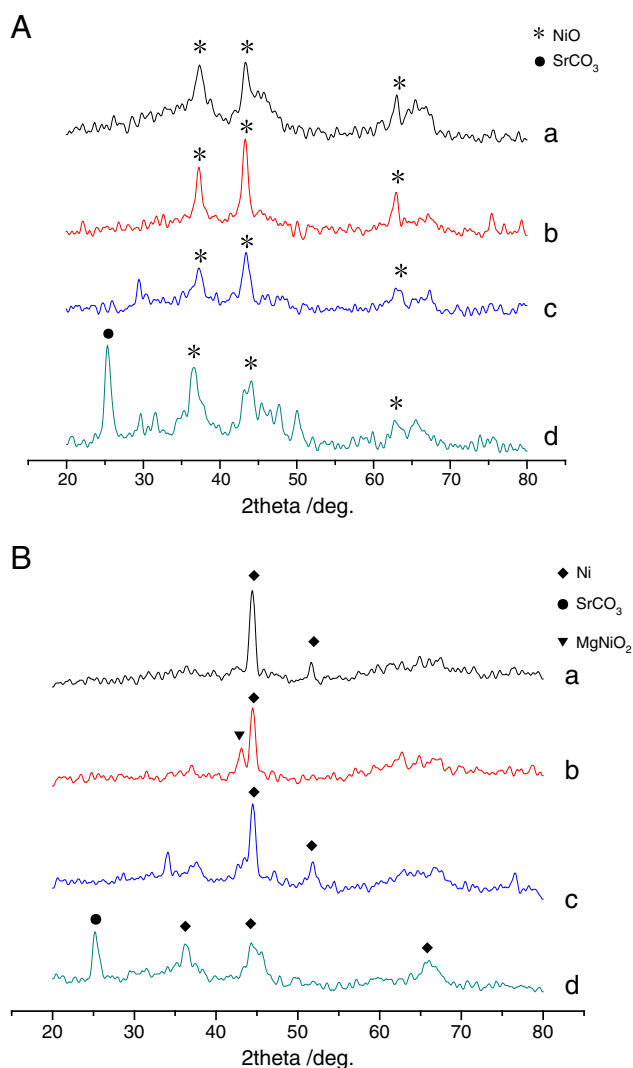
Fig. 1. XRD patterns of the nickel-based catalysts before (A) and after (B) reduction (a: Ni/γ-Al$_2$O$_3$; b: Ni–Mg/γ-Al$_2$O$_3$; c: Ni–Ca/γ-Al$_2$O$_3$; d: Ni–Sr/γ-Al$_2$O$_3$).
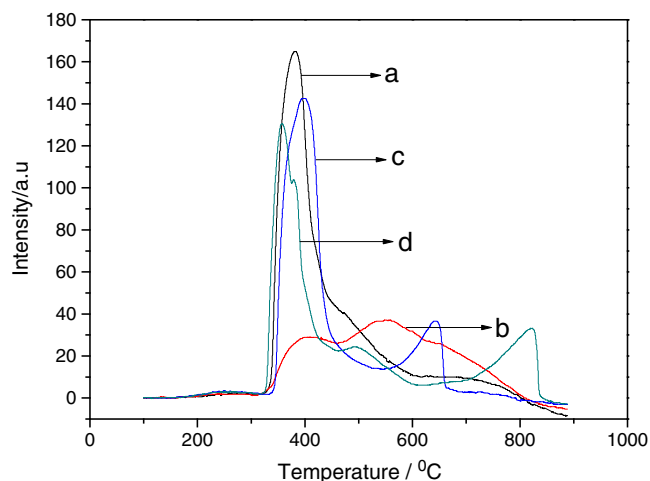
Fig. 2. TPR profiles of the nickel-based catalysts. (a: Ni/γ-Al$_2$O$_3$; b: Ni–Mg/γ-Al$_2$O$_3$; c: Ni–Ca/γ-Al$_2$O$_3$; d: Ni–Sr/γ-Al$_2$O$_3$.)

reactor. Prior to the reaction, catalysts were all pretreated under hydrogen at 450 °C for 3 h. Ten weight percent hydroquinone ethanol solution was dosed into the reactor at a speed of 0.3 mL/min by a micro syringe pump. Reaction mixtures were analyzed by a gas chromatograph using a 30 m SE-54 capillary column and the product structures were confirmed by a gas chromatography–mass spectroscopy (GC–MS) on Agilent 5975C.

3. Results and discussion

3.1. Catalyst characterizations

Table 1 shows some information about physicochemical properties of the nickel-based catalysts. It was found that the surface areas of the nickel-based catalysts were all above 130 m^2/g and the average pore sizes were all in the range of about 5 to 6 nm. It was noticeable that surface areas of catalysts were all increased and the pore sizes decreased after the addition of the alkaline earth metals. Furthermore, the addition of the alkaline earth metals are proved to be in favor of the Ni dispersion, especially for Sr; thus the Ni–Sr/γ-Al$_2$O$_3$ catalyst had the smallest Ni particle sizes among the four catalysts studied [12].
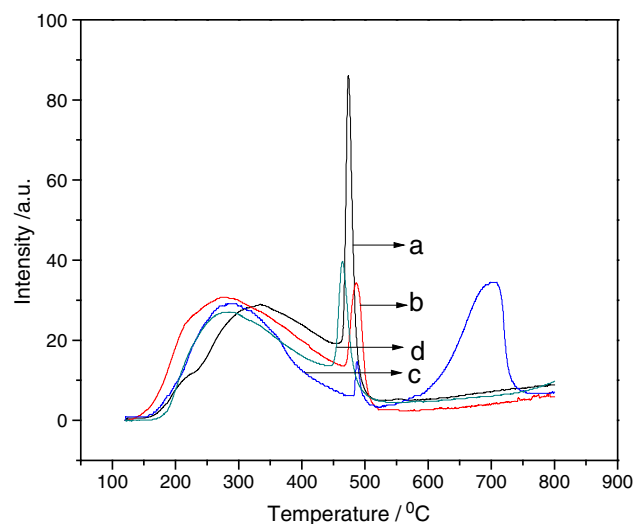
Fig. 3. NH$_3$-TPD profiles of the nickel-based catalysts. (a: Ni/γ-Al$_2$O$_3$; b: Ni–Mg/γ-Al$_2$O$_3$; c: Ni–Ca/γ-Al$_2$O$_3$; d: Ni–Sr/γ-Al$_2$O$_3$.)

A

B
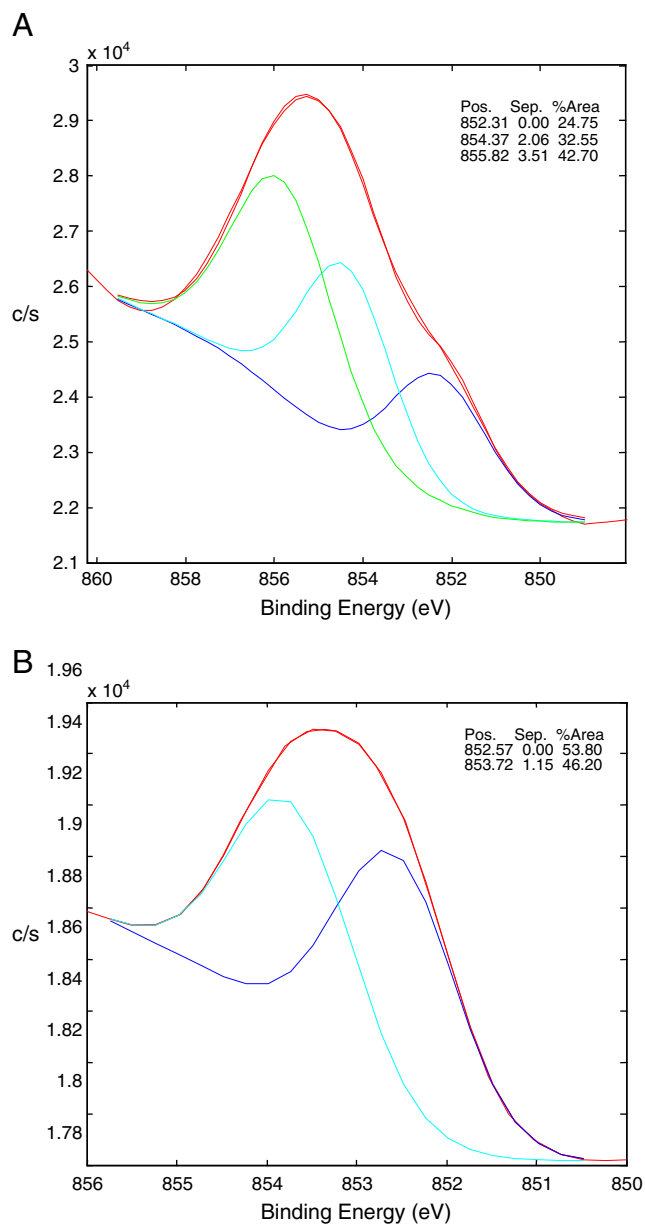
Fig. 4. XPS spectra of Ni/γ-Al₂O₃ catalyst (A) and Ni–Sr/γ-Al₂O₃ catalyst (B).

XRD patterns of the nickel-based catalysts are shown in Fig. 1. As can be seen, all samples before reduction presented the peaks characteristic of NiO at about 43° (Fig. 1A). In addition, in the case of the Ni–Sr/γ-Al₂O₃ catalyst, a SrCO₃ phase was clearly detected at about 25°. The

Ni–Sr/γ-Al₂O₃ catalyst had the smallest crystallite size among the four catalysts studied (Table 1), which indicated the Ni species were in a highly dispersed state in this catalyst, as also shown by SEM images. New peaks corresponding to Ni⁰ were clear in the XRD patterns of the reduced samples (Fig. 1B), which implied that NiO was reduced to metallic Ni during the reduction process and Ni⁰ is the active species in the reduced catalysts. Furthermore, SrCO₃ was also detected from the reduced Ni–Sr/γ-Al₂O₃ catalyst. The crystallite sizes of all modified catalysts except the Sr doped sample were found to be remarkably larger, which may be due to the agglomeration during the reduction process. We assumed that the SrCO₃ in the Ni–Sr/γ-Al₂O₃ catalyst was highly stable, and then prevented the active Ni species from agglomeration during the reduction process.

TPR profiles of the nickel-based catalysts are shown in Fig. 2. One main reduction peak was observed at around 400 °C in the profiles of the nickel-based catalysts except the Ni–Mg/γ-Al₂O₃ catalyst. In the case of Ni–Mg/γ-Al₂O₃ catalyst, there were three reduction peaks centered at about 400, 550 and 650 °C, which were assigned to the reduction of the bulk NiO, the highly dispersed Ni^{2+} species and the MgNiO₂[13]. Furthermore, there was one moderate peak centered at about 650 °C in the Ni–Ca/γ-Al₂O₃ catalyst, and one moderate peak centered at about 800 °C in the Ni–Sr/γ-Al₂O₃ catalyst, together with a small peak at about 500 °C. It was reported that the reduction peaks below 500 °C can be ascribed to the reduction of the bulk NiO in the nickel-based catalysts, and the reduction peaks in the region of 500 °C–700 °C can be ascribed to the reduction of the highly dispersed Ni^{2+} species in strong interaction with the supports [14]. Moreover, the peak at 800 °C in the Ni–Sr/γ-Al₂O₃ catalyst was suggested to be the reduction of SrCO₃. The disappearance of the SrCO₃ characteristic peak and the appearance of a new peak corresponding to Sr on the XRD curve of the reduced Ni–Sr/γ-Al₂O₃ catalyst after the TPR test can support this assumption. The existence of SrCO₃ may enhance the dispersion of metallic Ni in the common reduced Ni–Sr/γ-Al₂O₃ catalyst. Noticeably, the Ni–Sr/γ-Al₂O₃ catalyst presented the lowest reduction temperature for the reduction of the bulk NiO among the four catalysts studied. Pillai and Sahle-Demessie [15] have reported that Sr is an electropositive metal and it can donate its outer electrons to other metal and make it more electronegative. This electronic effect may increase the reducibility of NiO in the Ni–Sr/γ-Al₂O₃ catalyst. Thus, it is reasonable that the Ni species are more reducible in the Ni–Sr/γ-Al₂O₃ catalyst and the metallic Ni exists in a highly dispersed state in the reduced catalyst.

NH₃-TPD profiles of the nickel-based catalysts are presented in Fig. 3. The strong peaks centered at 250 °C–350 °C can be assigned to the weak acidic sites in all the catalysts. It is noticeable that the Ni–Sr/γ-Al₂O₃ catalyst showed both lower desorption temperature and smaller amount of weak acidic sites than the Ni/γ-Al₂O₃ catalyst. NH₃-TPD profiles of the four catalysts also showed one remarkable desorption peak at 480 °C–520 °C, which can be assigned to the moderate acidic sites [16]. It is clear that the Ni–Sr/γ-Al₂O₃ catalyst had lower desorption temperatures and areas than the Ni–Mg/γ-Al₂O₃ and Ni/γ-Al₂O₃

Table 2
Catalytic performances of the nickel-based catalysts[a].

Catalyst	Molar ratio (X/Ni)[b]	Conversion (%)	Selectivities (%)			
			1,4-Cyclohexanediol	Phenol	Cyclohexanol	4-Ethyl-cyclohexanone
Ni/γ-Al₂O₃	0	90.8	69.9	13.4	14.9	1.8
Ni–Mg/γ-Al₂O₃	0.25	86.8	73.7	17.2	7.0	2.1
Ni–Ca/γ-Al₂O₃	0.25	82.5	54.0	37.8	4.9	3.3
Ni–Sr/γ-Al₂O₃	0.25	92.6	91.6	3.8	3.0	1.6
Ni–Sr/γ-Al₂O₃	1	55.9	100	0	0	0
Ni–Sr/γ-Al₂O₃	0.5	70.0	97.4	0	2.6	0
Ni–Sr/γ-Al₂O₃	0.4	92.1	96.8	2.0	1.0	0.2
Ni–Sr/γ-Al₂O₃	0.3	91.0	93.4	2.7	3.7	0.2

[a] Reaction conditions: hydrogen pressure = 1.5 MPa; reaction temperature = 160 °C; flow rate of hydroquinone ethanol solution = 0.3 mL/min.
[b] X = Mg, Ca, Sr.
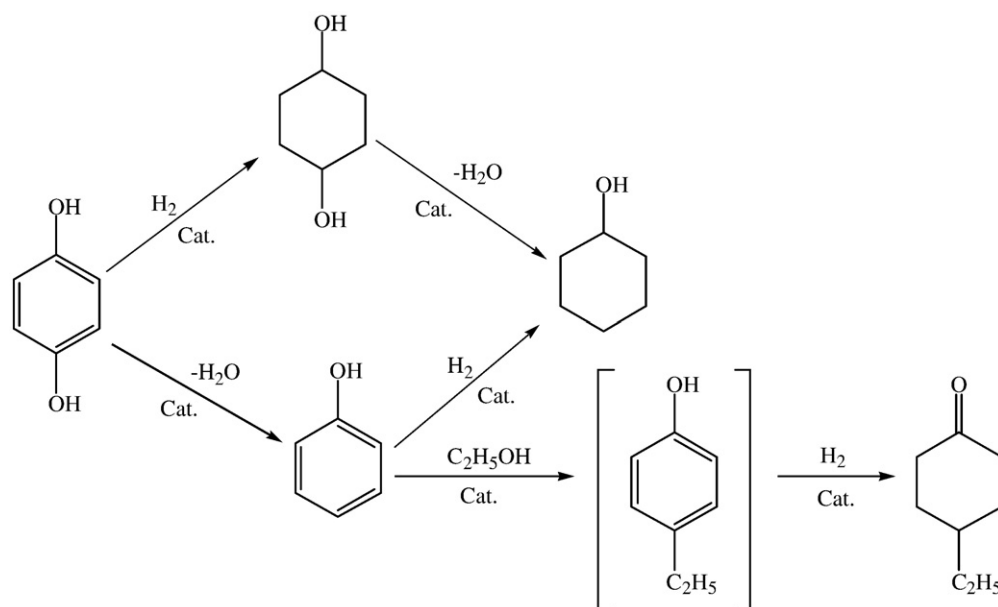
Scheme 1. Proposed routes for hydroquinone hydrogenation.

catalysts, but higher areas than the Ni–Ca/γ-Al$_2$O$_3$ catalyst for this desorption peak, whereas only the Ni–Ca/γ-Al$_2$O$_3$ sample showed one obvious high-temperature desorption peak at 600 °C–730 °C, which can be ascribed to the strong acidic sites. Thus, it can be concluded that the Ni–Sr/γ-Al$_2$O$_3$ catalyst had the lowest amounts of the weak and total acidic sites among the four catalysts studied.

The surface electronic states of Ni in the nickel-based catalysts are determined by XPS. By applying the curve fitting procedure, Ni^0 and Ni^{2+} were both detected on the surface of the reduced catalysts (Fig. 4). The amount of Ni^0 was 53.8% on the surface of the reduced Ni–Sr/γ-Al$_2$O$_3$ catalyst, whereas it was only 24.8% on the surface of the reduced Ni/γ-Al$_2$O$_3$ catalyst; thus the reduced Ni–Sr/γ-Al$_2$O$_3$ catalyst was proved to have more surface Ni^0 than the reduced Ni/γ-Al$_2$O$_3$ catalyst even though it has less surface Ni species (Table 1). The above observation and the fact that Ni^0 is the major phase in the body of reduced catalysts based on the XRD characterization can confirm that Ni^0 is the active site for the reduced catalysts.
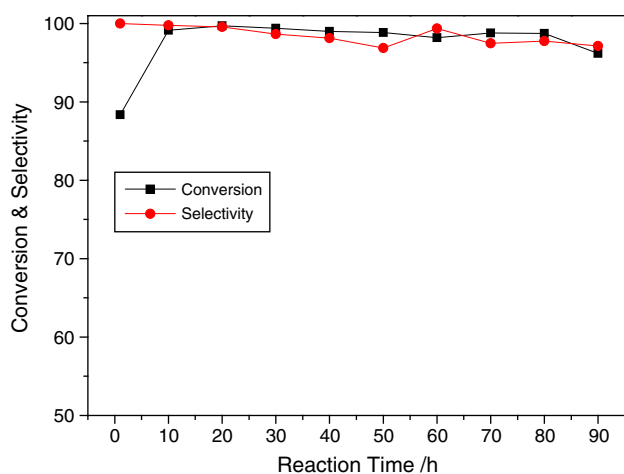
Fig. 5. Service life of the Ni–Sr/γ-Al$_2$O$_3$ catalyst. (Reaction conditions: hydrogen pressure = 2.0 MPa; reaction temperature = 160 °C; flow rate of hydroquinone ethanol solution = 0.3 mL/min.)

3.2. Catalytic performance

A series of nickel-based catalysts with 20 wt% Ni were prepared and tested on the continuous hydrogenation of hydroquinone in a fixed-bed reactor. Results are listed in Table 2. The Ni/γ-Al$_2$O$_3$ catalyst without any addition showed a good conversion (90.8%), but the selectivity to 1,4-cyclohexanediol was relatively low (69.9%). GC–MS analysis showed the main by-products were phenol and cyclohexanol, which were mainly from the dehydration of hydroquinone and 1,4-cyclohexanediol (Scheme 1). The catalytic performance of the Mg and Ca promoted samples was even worse. Both the conversion and the selectivity to 1,4-cyclohexanediol was decreased in the Ni–Ca/γ-Al$_2$O$_3$ catalyst, and the selectivity to phenol was nearly three times than that of the Ni/γ-Al$_2$O$_3$ catalyst. This may be due to the existence of strong acidic sites for this catalyst, which will enhance the dehydration of hydroquinone. Fortunately, the Ni–Sr/γ-Al$_2$O$_3$ catalyst showed the best performance among the catalysts studied. The conversion of hydroquinone was 92.6% and the selectivity to 1,4-cyclohexanediol was 91.6%, with the ratio of the cis- and trans-1,4-cyclohexanediol being about 3 to 1. Considering that the acidic sites can cause the dehydration of the –OH group [9,10,17], the addition of Sr was believed to suppress the dehydration process and enhance the selectivity to the desired product. The effect of Sr/Ni molar ratio was further investigated to achieve a better performance (Table 2, entries 5–8). It is found that the selectivities to 1,4-cyclohexanediol increased with the increase of the Sr/Ni molar ratio and the Ni–Sr/γ-Al$_2$O$_3$ catalyst with the Sr/Ni molar ratio of 0.4 showed the best performance, with the conversion of hydroquinone being 92.1% and the selectivity to 1,4-cyclohexanediol being 96.8%. Thus, Ni–Sr/γ-Al$_2$O$_3$ was chosen as the catalyst for the hydrogenation of hydroquinone to produce 1,4-cyclohexanediol. Finally, a service life test was performed under the optimum reaction conditions: hydrogen pressure, 2.0 MPa; reaction temperature, 160 °C; flow rate of hydroquinone ethanol solution, 0.3 mL/min. The Ni–Sr/γ-Al$_2$O$_3$ catalyst showed excellent stability during the 90 h test (Fig. 5). The conversion of hydroquinone first increased from 88.4% to 99.2% during the first 10 h and then kept stable, implying that the catalyst needs a preliminary activation before it reaches the best activity. On the other hand, the selectivity to 1,4-cyclohexanediol remained above 96.7% during the whole test. Thus, the total yield of 1,4-cyclohexanediol is over 95.0% after the

preliminary 10 h of activation, which is higher than the reported yields in previous works.

4. Conclusion

A continuous process for the highly selective synthesis of 1,4-cyclo-hexanediol via the hydrogenation of hydroquinone using nickel-based catalysts is first established in this paper. A Ni–Sr/γ-Al$_2$O$_3$ catalyst was found to have the best activity and selectivity among the catalysts studied. The conversion of hydroquinone was 99.2% under the optimal reaction conditions and the selectivity to 1,4-cyclohexanediol remained above 96.7% during the 90 h service life test over this catalyst. The more active Ni^0 on its surface is believed to be responsible for its high activity and the weak acidity, caused by the formation of SrCO$_3$, favors its high selectivity to 1,4-cyclohexanediol. Due to its good activity and stability, this continuous process involving a Ni–Sr/γ-Al$_2$O$_3$ catalyst is not only economically viable but also potentially applicable to large-scale reactions.

Acknowledgements

Appendix A. Supplementary data

Supplementary data to this article can be found online at doi:10. 1016/j.catcom.2011.10.026.

References

[1] A.M. Galal, W. Gul, D. Slade, S.A. Ross, S.X. Feng, Bioorganic & Medicinal Chemistry 17 (2009) 741–751.
[2] R.J. Crawford, Journal of Organic Chemistry 48 (1983) 1366–1368.
[3] H. Adkins, H.I. Cramer, Journal of the American Chemical Society 52 (1930) 4349–4358.
[4] H. Adkins, H.R. Billica, Journal of the American Chemical Society 70 (1948) 695–698.
[5] L.J. Gillespie, T.H. Liu, Journal of the American Chemical Society 53 (1931) 3969–3972.
[6] E.J. Shin, M.A. Keane, Industrial and Engineering Chemistry Research 39 (2000) 883–892.
[7] S.G. Shore, E. Ding, C. Park, M.A. Keane, Journal of Molecular Catalysis A: Chemical 212 (2004) 291–300.
[8] T. Ushikubo, K. Wada, Journal of Catalysis 148 (1994) 138–148.
[9] Á. Molnár, K. Felföldi, M. Bartók, Tetrahedron 37 (1981) 2149–2151.
[10] Á. Molnár, M. Bartók, Reaction Kinetics and Catalysis Letters 4 (1976) 315–321.
[11] H.B. Cho, J.H. Park, B.E. Hong, Y.H. Park, Bulletin of the Korean Chemical Society 29 (2008) 328–334.
[12] Z.J. Wu, Z.F. Zhao, M.H. Zhang, ChemCatChem 2 (2010) 1606–1614.
[13] M. Serra, P. Salagre, Y. Cesteros, F. Medina, J.E. Sueiras, Journal of Catalysis 197 (2001) 210–219.
[14] J. Xiong, J.X. Chen, J.Y. Zhang, Catalysis Communications 8 (2007) 345–350.
[15] U.R. Pillai, E. Sahle-Demessie, Applied Catalysis A: General 281 (2005) 31–38.
[16] G.Y. Bai, H.Y. Dou, M.D. Qiu, X.X. Fan, F. He, L.B. Niu, Catalysis Letters 138 (2010) 187–192.
[17] V.Z. Fridman, A.A. Davydov, Journal of Catalysis 195 (2000) 20–30.